A mechanism that accounts for the observed behavior of the cyclopropenone ketals is detailed in Scheme I. Nucleophilic attack of the strained cyclopropene olefin onto the electron-deficient olefin, rearrangement of the cyclopropyl cation to the allyl cation, and subsequent collapse of the dipole affords the observed products. The results of an initial study on the reactivity and behavior of cyclopropenone ketals by Albert and Butler[5b] and preliminary results of our own[8] are suggestive that such a mechanism is operative.

Investigations to determine the full scope of these observations are in progress.

Acknowledgment. This work was assisted financially by the Chicago Community Trust Co./Searle Scholars Program, the National Institutes of Health (CA 00898, GM 07775), and donors of the Petroleum Research Fund, administered by the American Chemical Society. We thank Dr. Cynthia S. Day of Crystalytics Co. for the prompt experimental treatment in the X-ray structure determination in **13**.

Registry No. 1, 60935-21-9; **2**, 85531-80-2; **3**, 88442-03-9; **4**, 88442-04-0; **5**, 5292-53-5; **6**, 6626-84-2; **7**, 1462-12-0; **8**, 22398-14-7; **9**, 2700-22-3; **10**, 88442-05-1; (±)-**11**, 88442-06-2; **12**, 88442-07-3; **13**, 88442-08-4; **14**, 88442-09-5; **15**, 88442-10-8; **16**, 88442-11-9; **17**, 88442-12-0.

Supplementary Material Available: Complete spectral information on **10–17** is listed and full details of the X-ray structure determination of **13** are provided (20 pages). Ordering information is given on any current masthead.

(8) Treatment of methyl methacrylate with **1** (benzene or dioxane, 70–75 °C, 12–24 h) apparently affords v, a highly unstable product that is the result

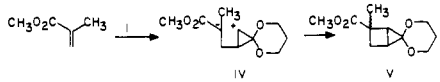

of [2 + 2] cycloaddition. This suggests that the dipolar intermediates ii are sufficiently stable and long-lived compared to iv to allow the cyclopropyl cation to allyl cation rearrangement (ii → iii) to precede collapse of the dipolar intermediates.

(9) Prepared from nopinone by the three-step procedure: (1) NaH, $CO(OEt)_2$, THF; (2) NaH, THF, PhSeBr; (3) H_2O_2, CH_2Cl_2–H_2O. We thank M. Patel for providing us with this sample.

Synthesis of Ligand-Free Transition-Metal Dihydrides in Low-Temperature Matrices: Manganese Dihydride, MnH_2

Geoffrey A. Ozin* and John G. McCaffrey

Lash Miller Chemistry Laboratories
University of Toronto
Toronto, Ontario, Canada M5S 1A1

Received July 21, 1983

There is a growing interest in ligand-free transition-metal dihydrides. This can be traced to their potential for modeling H_2 chemisorption on metal surfaces,[1] for probing H_2 oxidative-addition reactions in homogeneous catalysis,[2] and for identifying metal hydride species in solar spectra from sunspots and stars.[3]

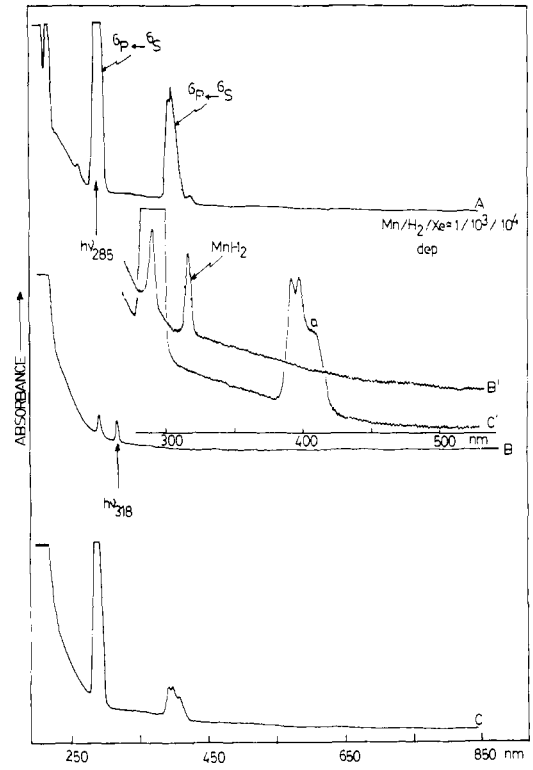

Figure 1. Optical spectra of (A) freshly deposited $Mn/H_2/Xe \simeq 1/10^3/10^4$ matrices at 10–12 K: (B) following 60 min of 285-nm photolysis of (A), (C) following 15 min of 318-nm photolysis of (B). B′ and C′ are approximately times 3 ordinate expansions of B and C, respectively.

The inherent molecular simplicity of MH_2 also makes them ideally suitable models for detailed spectroscopic and structural investigations backed by quantum chemical calculations.[4]

The available experimental data for ligand-free transition-metal dihydrides is, however, extremely sparse, probably because of their transient nature, high reactivity, and lack of convenient syntheses. Only metal atom–hydrogen atom matrix cocondensations have previously been demonstrated to lead to MH_x species. This method yields mixtures of metal hydrides (x = 1, 2, 3; M = Cr, Mn) coisolated with H and H_2 products.[5] Aside from spectroscopic complications, such mixtures would make subsequent studies of the chemistry of the ligand-free MH_x species with other coadded ligands, like CO, N_2, C_2H_4, difficult.

In this communication we wish to report on a new method for fabricating ligand-free transition-metal dihydrides in low-temperature matrices, completely devoid of H atoms and other MH_x products. The method involves resonance excitation of metal atoms coisolated with H_2 in rare gas matrices at 10–12 K. In this paper the metal atom photochemical technique is demonstrated by reference to Mn atoms in 10% H_2/Xe matrices. This choice was predicated on the inherent simplicity of the electronic ground state of Mn atoms $^6S_{5/2}(3d^54s^2)$ and its associated atomic resonance spectrum[6] (Figure 1A) as well as the existence of an earlier literature claim for the matrix synthesis of MnH_2 from Mn atom–H atom cocondensations in Xe, therefore permitting cross comparisons between the two different approaches. The use of high H_2 concentrations in Xe was designed to favor the formation of the highest possible stoichiometry manganese hydride, while

(1) Bates, G.; Katzer, J. R.; Schmit, G. C. A. "Chemistry of Catalytic Processes"; McGraw-Hill: New York, 1979; "The Nature of the Surface Chemical Bond"; Rhodin, T. N., Ertl, G., Eds.; North-Holland: Amsterdam, 1979; and references cited therein.

(2) Collman, J. P.; Hegedus, L. S. "Principles and Applications of Organotransition Metal Chemistry"; University Science Books: Mill Valley, CA. Parshall, G. W. "Homogeneous Catalysis"; Wiley-Interscience: New York, 1980; and references cited therein.

(3) Wing, R. F.; Cohen, J.; Brautt, J. W. *Astrophys. J.* **1977**, *216*, 659. Mould, J. R.; Wyckoff, S. *M.N.R.A.S.* **1978**, *182*, 63 and references cited therein.

(4) Blomberg, M. R. A.; Siegbahm, Per. E. M. *J. Chem. Phys.* **1983**, *78*, 5682. Tyrrell, J.; Youakim, A. *J. Phys. Chem.* **1980**, *84*, 3568; 1981, *85*, 3614, and references cited therein.

(5) Van Zee, R. J.; DeVore, T. C.; Wilkerson, J. L.; Weltner, W., Jr. *J. Chem. Phys.* **1978**, *69*, 1869. Van Zee, R. J.; DeVore, T. C.; Weltner, W., Jr. *J. Chem. Phys.* **1979** *71*, 2051.

(6) Klotzbücher, W.; Ozin, G. A. *Inorg. Chem.* **1980**, *19*, 3776 and references cited therein.

0002-7863/84/1506-0807$01.50/0

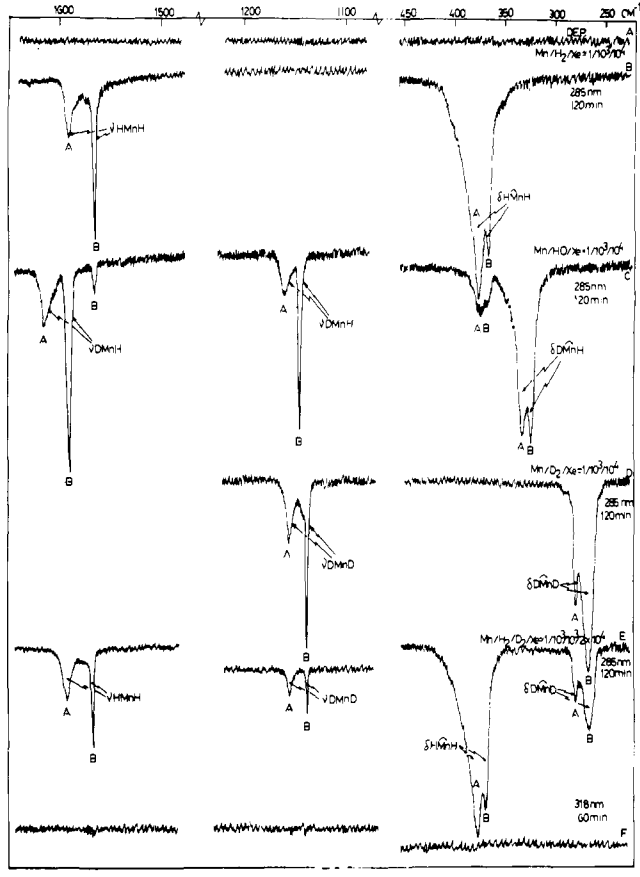

Figure 2. Infrared spectrum of (A) freshly deposited $Mn/H_2/Xe \simeq 1/10^3/10^4$ matrices at 10–12 K (B): following 60 min of 285-nm photolysis of (A), (C) the same as (B) but for $Mn/HD/Xe \simeq 1/10^3/10^4$, (D) the same as (B) but for $Mn/D_2/Xe \simeq 1/10^3/10^4$, (E) the same as (B) but for $Mn/H_2/D_2/Xe \simeq 1/0.5 \times 10^3/0.5 \times 10^3/10^4$, (F) following 20 min of 318-nm photolysis of (B).

at the same time minimizing competing Mn atom photoaggregation processes toward low-nuclearity Mn_x clusters.

Thus, when the $^6P(3d^54s^14p^1) \leftarrow {}^6S(3d^54s^2)$ transition of atomic Mn is excited by narrow-band (20-nm or 8-nm bwhh) 285-nm irradiation (450-W Xe lamp, monochromator, 10-cm water cell assembly delivering around 100 $\mu W\ cm^{-2}$ at the sample at 280–320 nm), one observes rapid decay of all of the Mn atom lines with concurrent growth of a new absorption centered around 315 nm (Figure 1B). Subsequent excitation into the low-energy side of the product band (318 nm, minimizes overlap with neighboring Mn atom lines) causes rapid bleaching of the 315-nm absorption with concurrent regeneration of the Mn atomic resonance lines (Figure 1C). Approximately 80% of the original Mn atoms can be recovered by this reverse photolysis (photoreductive-elimination) procedure.

The infrared spectra of samples corresponding to the optical traces shown in Figure 1A–C reveal the growth of manganese–hydrogen stretching and deformational modes centered around 1591, 1565 cm^{-1} and 375, 366 cm^{-1}, respectively, following 285-nm Mn atom photolysis (Figure 2B), which can be annihilated by 318-nm photolysis (Figure 2F). This is in line with the corresponding behavior observed by optical spectroscopy (vida infra). Thermal annealing studies of these H_2/Xe matrices indicates that the manganese hydride products fall into two distinct categories denoted A and B and absorbing at 1591 and 375 cm^{-1} and 1565 and 366 cm^{-1}, respectively. The latter species appears to be favored. The corresponding infrared experiments performed with $D_2/Xe \simeq 1/10$, $HD/Xe \simeq 1/10$, and $H_2/D_2/Xe \simeq 1/1/20$ matrices reveal isotopic patterns (Figure 2C–E) in the manganese–hydrogen stretching and deformation regions characteristic of a manganese dihydride, with no spectroscopic evidence for MnH,[5] and MnH_x ($x \geq 3$), $Mn(H_2)$ (molecular dihydrogen complexes), or $Mn^+(H_2^-)$ ion pairs (Table I).[7] The lack of

Table I. Infrared Spectra of Manganese Dihydride in Solid Xenon

MnH_2	MnHD	MnD_2	mode assignment[a]
	1618		ν(MnH), A
	1588		ν(MnH), B
1591			ν(MnH), A
1565			ν(MnH), B
	1160		ν(MnD), A
	1144		ν(MnD), B
		1154	ν(MnD), A
		1137	ν(MnD), B
375			$\delta(MnH_2)$, A
366			$\delta(MnH_2)$, B
	334		δ(MnHD), A
	324		δ(MnHD), B
		276	$\delta(MnD_2)$, A
		266	$\delta(MnD_2)$, B

[a] Species B favored on thermal annealing at 20 K.

evidence for H/D scrambling processes in the $H_2/D_2/Xe$ experiments (only $MnH_2 + MnD_2$, no MnHD) provides evidence for a concerted insertion of Mn into H_2. Furthermore, the preferential formation of MnH_2 over that of MnD_2 in $H_2/D_2/Xe \simeq 1/1/20$ matrices by a factor of around 3 (infrared absorbance ratio for MnD_2 and MnH_2 stretching and deformational modes)[8] alerts one to the existence of an activation barrier for the insertion step.[9]

It is interesting to note that of the two forms of MnH_2 that can be photochemically generated in this study, it is the A form of MnH_2 that can be identified with the MnH_2 product claimed from the Mn atom/H atom/Xe matrix work. One can surmise that the matrix cage requirements are different for the two modes of formation of MnH_2

$$Mn \xrightarrow[12\ K]{H} MnH \xrightarrow[12\ K]{H} MnH_2$$

$$Mn + H_2 \xrightarrow[12\ K]{h\nu} MnH_2$$

and it is therefore not too surprising that MnH_2 can be formed

(7) The IR isotopic pattern for species A and B in H_2, D_2, and HD xenon matrices (Figure 2) cannot be fit to either MnH/MnD or $MnH_3/MnH_2D/MnHD_2/MnD_3$ or a higher stoichiometry manganese hydride species. It can be satisfactorily assigned to MnH_2, MnD_2, and MnHD as indicated in Table I. Although the molecular hydrogen complexes $Mn(H_2)$, $Mn(D_2)$, and Mn(HD) could conceivably produce an isotopic pattern like the one observed, the absence of a high-frequency hydrogen–hydrogen stretching mode in the 4400–2000-cm^{-1} range (which is observed for $W(CO)_3(P\text{-}i\text{-}Pr_3)_2(\eta^2\text{-}X_2)$ ($X_2 = H_2$, D_2, HD): Kubas, G. J.; Ryan, R. R.; Swanson, B. I.; Vergamini, P. J.; Wasserman, H. *J. Am. Chem. Soc.*, submitted for publication) argues against this kind of assignment.

(8) Note that the ratio of the IR intensities of the asymmetric stretching modes for MnH_2 and MnD_2 isotopic molecules is given by

$$I_H/I_D = (M_{Mn} + 2M_H \sin^2(\theta/2))/(M_{Mn} + 2M_D \sin^2(\theta/2))$$

where θ is the apical angle and M_i is the atomic weight of atom i (bond dipole approximation, neglecting coupling with the bending mode: "Molecular Vibrations"; Wilson, E. B.; Jr., Decius, J. C., Cross, P. C. Eds.; McGraw-Hill: New York, 1955; p 191). For θ in the range 180–90°, this translates into a correction of 3–2%, respectively, in the absorbance ratio of the asymmetric manganese–hydrogen stretching modes of MnH_2/MnD_2.

(9) Note that for a pseudo-first-order competitive insertion reaction, $Mn^* + H_2 + D_2 \rightarrow MnH_2 + MnD_2$, the time dependence of the concentration of the MnH_2 and MnD_2 photoproducts (IR) is given by

$$[MnH_2] = \left[\frac{k_H}{k_H + k_D}\right][Mn_0](1 - \exp[-\tfrac{1}{2}(k_H + k_D)t])$$

$$[MnD_2] = \left[\frac{k_D}{k_H + k_D}\right][Mn_0](1 - \exp[-\tfrac{1}{2}(k_H + k_D)t])$$

which leads in one experiment directly to $k_H/k_D = [MnH_2]/[MnD_2]$. Taking into account the low temperature at which the reaction is performed (zero point energy and possibly tunneling corrections), we observe a k_H/k_D isotope ratio of around 3 for the $Mn^*/H_2/D_2$ reaction which translates into a k_H/k_D ratio of about 1.05–1.08 at ambient temperatures, which would indicate a small degree of H–H stretching in an "early" transition state and probably a low activation barrier for the insertion reaction.

in different matrix cages with MnH_2 possibly immobilized with slightly different structures.[10,11]

Acknowledgment. The financial assistance of the Natural Sciences and Engineering Research Council of Canada's Operating and Strategic grants programmes is greatly appreciated.

Registry No. MnH_2, 13767-07-2; MnHD, 88392-37-4; MnD_2, 88392-36-3; Mn, 7439-96-5; H_2, 1333-74-0; HD, 13983-20-5; D_2, 7782-39-0; Xe, 7440-63-3; Ar, 7440-37-1.

(10) It is not possible from the IR data to make a definitive statement at this time concerning the structure of MnH_2 in Xe. All that one can say, is that the two slightly different forms of MnH_2 in Xe (multiple-site effect or geometrical isomers) display no evidence for a symmetrical IR active $\nu(MnH_2)$ stretching mode. This could be taken to indicate linearity for both forms. However, caution must be exercised here, as the sym $\nu(MnH_2)$ mode of a bent MnH_2, B molecule could be overlapped by the asym $\nu(MnH_2)$ mode of the A form, and/or A and B might be only slightly bent yielding an IR sym $\nu(MnH_2)$ band that remains below the detection limit of our experiment. Raman data will help clarify this important point.

(11) MnH_2 can also be generated in solid Ar by using similar experimental techniques.

Displacement, Proton Transfer, or Hydrolysis? Mechanistic Control of Acetonitrile Reactivity by Stepwise Solvation of Reactants

Gary Caldwell, Melvin D. Rozeboom, Jeffery P. Kiplinger, and John E. Bartmess*

Department of Chemistry, Indiana University Bloomington, Indiana 47405

Received September 8, 1983

The absence of solvation can drastically alter many ionic reaction mechanisms from that which occurs in solution. There are several recent reports of mechanistic changeovers from solution to gas phase occurring on detachment of the last molecule of solvent from the reactive ion.[1] We report here what is to our knowledge the first case where three distinct reactivity pathways occur upon stepwise solvation: bare, monosolvated, and bulk-solvated hydroxide ion react with acetonitrile to give three different sets of products.

As part of a general study of the formation, thermochemistry, and reactivity of monosolvated anions,[2] we have examined the reactions of a number of carbon acids with species such as $RO^-\cdot\cdot HOR$ in our ICR spectrometer.[3] Ketones, aldehydes, and acetylenes readily exchange into such alcohol–alkoxide species to give ions corresponding in mass to the deprotonated carbon acid solvated by the alcohol.[1b,c] Further reactions of such species are consistent with such a structure: either the solvent alcohol or the carbon acid can undergo further switching reactions with other alcohols, and the threshold for the carbon acid switching into the monosolvated ion is consistent with its acidity.[4]

When acetonitrile, water, and dimethylformamide are present in the ICR spectrometer, monosolvated hydroxide produced by the reaction sequence (1)–(4) reacts to form an ion of mass 58,

$$H_2O + e^- (6.2\ eV) \rightarrow H^- + HO\cdot \quad (1)$$

$$H^- + H_2O \rightarrow HO^- + H_2 \quad (2)$$

$$HO^- + HCONMe_2 \rightarrow HOH\cdot\cdot{}^-NMe_2 + CO \quad (3)$$

$$HOH\cdot\cdot{}^-NMe_2 + H_2O \rightarrow HOH\cdot\cdot{}^-OH + HNMe_2 \quad (4)$$

corresponding to $CH_2CN^-\cdot\cdot HOH$. No such product is observed when acetonitrile is absent or when $MeO^-\cdot\cdot HOMe$, formed by the Riveros reaction of MeO^- with HCO_2Me, analogously to (3), reacts with acetonitrile. The differing reactivity of the ions $HO^-\cdot\cdot HOH$ and $MeO^-\cdot\cdot HOMe$ would seem to denote a thermochemical threshold. However, acetonitrile reacting with $MeO^-\cdot\cdot HOH$ (from HO^- and HCO_2Me) gives a product of mass 58, corresponding to $CH_2CN^-\cdot\cdot HOH$, but no 72. This latter ion would be the methanol-solvated product $CH_2{=}C{=}N^-\cdot\cdot HOMe$ and should be prefered thermochemically, methanol being more acidic than water and therefore a better hydrogen bond donor. We believe that reaction 5 has occurred, involving an internal S_N2

$$CH_3CN + HO^-\cdot\cdot HOH \rightarrow CH_3OH\cdot\cdot{}^-CN + HOH \quad (5)$$

reaction, rather than a simple proton transfer and solvent switching, based on the following facts: (1) The pattern of reaction, with $HO^-\cdot\cdot HOH$ but not with $MeO^-\cdot\cdot HOMe$, is observed only for the carbon acid with a reasonably good leaving group, CN^-, and not for those carbon acids, such as acetone or acetophenone, of comparable acidity but with poor leaving groups. (2) The displacement mechanism explains the lack of the 72^- ion on reaction with $MeO^-\cdot\cdot HOH$; if methoxide is the nucleophile, the product would be dimethyl ether, which cannot hydrogen bond to cyanide like methanol can. (3) If various alcohols such as ethanol are present with the 58^- species, signals corresponding in mass to $MeOH\cdot\cdot{}^-OR$ and $ROH\cdot\cdot{}^-CN$ are observed, but none for $CH_2CN^-\cdot\cdot HOR$, though all these reaction products should be formed exothermically. (4) Addition of CO_2 to 58^- results in a product at the mass of $MeOCO_2^-$, but none for $HOCO_2^-$ or $NCCH_2CO_2^-$. We thus conclude that the methyl cation transfer, rather than proton transfer, is the principal mode of reaction.

The trifold pathways can be rationalized on the basis of the nature of the solvation. In general, transition states with diffuse charge are most favored in the absence of solvent, while charge localization results in better solvation and more stabilization in condensed protic media. For bare hydroxide reacting with the nitrile, deprotonation (−18.7 kcal/mol) and displacement of cyanide (−14.6 kcal/mol) are both exothermic. The preference for proton transfer must therefore reflect a rate phenomenon. The transition state for deprotonation should involve a looser complex, **1**, than the transition state for displacement, **2**, since the bonding

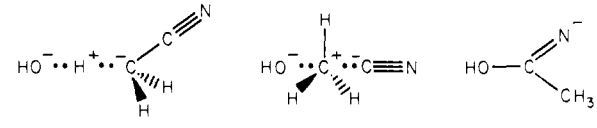

1 **2** **3**

is centered about an s rather than a p orbital on the transferred cation.[6] While the thermochemistry of simple addition of hydroxide to form the imide **3** is not known, the fact that it is an addition, with no fragment to bear away any excess energy, makes its observation unlikely under the conditions in the ICR spectrometer.[1d]

For the solution-phase counterparts of these processes, in protic solvents a slow hydrolysis ($k = 3 \times 10^{-6}\ M^{-1}\ s^{-1}$ at 35 °C) is observed.[7] Deuterium exchange catalyzed by DO^- occurs at "30–40 times" the hydrolysis rate.[8] In the solution phase, the attacking hydroxide should be well solvated by a protic solvent, while the transition states **1** and **2**, where the charge is more

(1) (a) Asubiojo, O. I.; Blair, L. K.; Brauman, J. I. *J. Am. Chem. Soc.* **1975**, *97*, 6685. (b) Comisarow, M. *Can. J. Chem.* **1977**, *55*, 171. (c) Fukuda, E. K.; McIver, R. T., Jr. *Ibid.* **1979**, *101*, 2498. (d) Bartmess, J. E. *J. Am. Chem. Soc.* **1980**, *102*, 2483.

(2) Caldwell, G.; Bartmess, J. E. *J. Am. Chem. Soc.*, submitted.

(3) McIver, R. T., Jr. *Rev. Sci. Instrum.* **1970**, *41*, 555; **1978**, *49*, 111. McIver, R. T., Jr.; Hunter, R. L.; Ledford, E. B., Jr.; Locke, M. J.; Francl, T. J. *Int. J. Mass Spectrom. Ion Phys.* **1981**, *39*, 65. Bartmess, J. E.; Caldwell, G. *Ibid.* **1981**, *41*, 125.

(4) Bartmess, J. E.; Scott, J. A.; McIver, R. T., Jr. *J. Am. Chem. Soc.* **1979**, *101*, 6046; **1979**, *101*, 6056. Bartmess, J. E.; McIver, R. T., Jr. In "Gas Phase Ion Chemistry"; Bowers, M. T., Ed.; Academic Press: New York, 1979, Chapter 11, *The Gas Phase Acidity Scale*.

(5) Kebarle, P. *Ann. Rev. Phys. Chem.* **1977**, *28*, 445.

(6) Farneth, W. E.; Brauman, J. I. *J. Am. Chem. Soc.* **1976**, *98*, 7891. Pellerite, M. J.; Brauman, J. I. *Ibid.* **1980**, *102*, 5993.

(7) Reitz, O. *Z. Phys. Chem., Abt. A* **1939**, *183*, 371. Rabinovitch, B. S.; Winkler, C. A. *Can. J. Res.* **1942**, *20B*, 185. Wideqvist, S. *Ark. Kemi* **1956**, *10*, 265. Schaefer, F. C.; Peters, G. A. *J. Org. Chem.* **1961**, *26*, 412.

(8) Bonhoeffer, K. F.; Geib, K. H.; Reitz, O. *J. Chem. Phys.* **1939**, *7*, 664.

0002-7863/84/1506-0809$01.50/0